Synchronized Andreev transmission in SNS junction arrays

N. M. Chtchelkatchev,[1,2,3] T. I. Baturina,[1,4,5] A. Glatz,[1] and V. M. Vinokur[1]
[1]*Materials Science Division, Argonne National Laboratory, Argonne, Illinois 60439, USA*
[2]*Institute for High Pressure Physics, Russian Academy of Sciences, Troitsk 142190, Moscow Region, Russia*
[3]*L. D. Landau Institute for Theoretical Physics, Russian Academy of Sciences, 117940 Moscow, Russia*
[4]*Institute of Semiconductor Physics, 13 Lavrentjev Avenue, Novosibirsk 630090, Russia*
[5]*Novosibirsk State University, 2 Pirogova Street, Novosibirsk, 630090, Russia*
(Received 8 June 2010; published 29 July 2010)

We construct a nonequilibrium theory for the charge transfer through a diffusive array of alternating normal (N) and superconducting (S) islands comprising an SNSNS junction, with the size of the central S island being smaller than the energy relaxation length. We demonstrate that in the nonequilibrium regime the central island acts as Andreev retransmitter with the Andreev conversions at both NS interfaces of the central island correlated via above-the-gap transmission and Andreev reflection. This results in a synchronized transmission at certain resonant voltages which in experiments is seen as a sequence of spikes in the differential conductivity.

DOI: 10.1103/PhysRevB.82.024526 PACS number(s): 74.45.+c, 73.23.−b, 74.78.Fk, 74.50.+r

I. INTRODUCTION

An array of superconductor (S)-normal metal (N) junctions offers a fundamental laboratory representing a wealth of physical systems and phenomena including Josephson-junction networks, disordered superconducting films, superconductor-insulator transition, and a rich variety of resonance effects utilizing the quantum coherence on a macroscale.[1] One of the fascinating examples of the latter is a recently reported anomalous enhancement of the charge transfer across the regular one- and two-dimensional SNS arrays at the values of the applied bias commensurate with the superconducting gap.[2–6] Electronic transport in these systems is mediated by Andreev conversion of a supercurrent into a current of quasiparticles and vice versa at the NS interfaces.[7] A benchmark of this mechanism is a multiple Andreev reflection (MAR),[8–10] the enhancement of the conductivity in a single SNS junction at voltages equal to an integer (m) fraction of the superconducting gap, $V=2\Delta/(em)$.[11–20] Experimental findings of Ref. 2 where high subharmonics, not visible in single SNS junctions, were observed brought about the concept of a *spatially distributed* Andreev reflection coherent on a macroscopic scale and posed a quest for a general theory of out-of-equilibrium large SNS networks.

The MAR process in a single diffusive SNS junction was studied in detail in Refs. 21 and 23. In this paper we show that wedging S_C into the normal part of an elemental SNS leads to nontrivial physics and the appearance of a new distinct resonant mechanism for the current transfer, *the synchronized Andreev transmission* (SAT), and construct a nonequilibrium theory for the current-voltage characteristics of such a composite SNSNS junction. A large array can be viewed as a system comprised of many SNSNS units, the behavior of which is thus a key element for the description of a large network, and, as we show below, the SAT-induced features become dominant in large arrays consisting of many SNS junctions.

II. QUALITATIVE PICTURE

In the SAT regime Andreev conversions at the boundaries of the central superconducting island are correlated: as a quasiparticle with energy ε hits one NS_C interface, a quasiparticle with the same energy emerges from the other S_CN interface into the bulk of the normal island (and vice versa, see Fig. 1). This energy synchronization is achieved via above-the-gap Andreev processes,[5] which align the MARs occurring in each of the normal islands and make the quasiparticle distribution at the central island essentially nonequilibrium. Effectiveness of the synchronization is controlled by the energy relaxation lengths of both, the quasiparticles crossing S_C with energies above Δ, and of quasiparticles experiencing MAR in the normal parts. The SAT processes result in spikes in the differential conductivity of the SNSNS circuit, which appear at resonant values of the *total* applied voltage V_{tot} defined by the condition

$$V_{tot} = 2\Delta/en \tag{1}$$

with integer n, irrespectively of the details of the distribution of the partial voltages at the two normal islands.

A recipe for determining resonant voltages of the SAT singularities can be derived from the space-energy diagrams (see Fig. 1). The figure presents main diagrams for the first and the second subharmonics, $n=1$ and $n=2$, with the ratio $R_1/R_2=3/4$, where R_1 and R_2 are the resistances of normal parts N_1 and N_2, respectively. This ratio results in the partial voltage drops $eV_1=6\Delta/7$ and $eV_2=8\Delta/7$ at $n=1$ [Figs. 1(a) and 1(b)], and $eV_1=3\Delta/7$ and $eV_2=4\Delta/7$ at $n=2$ [Figs. 1(c)–1(f)]. Note that these partial voltage drops are not MAR matching voltages of individual $S_LN_1S_C$ or $S_CN_2S_R$ parts. For the first subharmonic [Fig. 1(a)] a quasiparticle departs from the left superconducting electrode with the energy $\varepsilon=-\Delta$ to traverse N_1, and the quasiparticle that starts from the central island S_C with the same energy as the incident one to take up upon the current across the island N_2, and hit S_R with the energy $\varepsilon=\Delta$ (the ABCD path). The corresponding path for the hole [Fig. 1(b)] is D′C′B′A′.

In general, trajectories yielding resonant voltages of Eq. (1) have the following structure: they start and end at the BCS quasiparticle density-of-states singular points ($\varepsilon=\pm\Delta$) of S_L, S_C, and S_R, contain the closed polygonal path, which include MAR staircases in the normal parts and

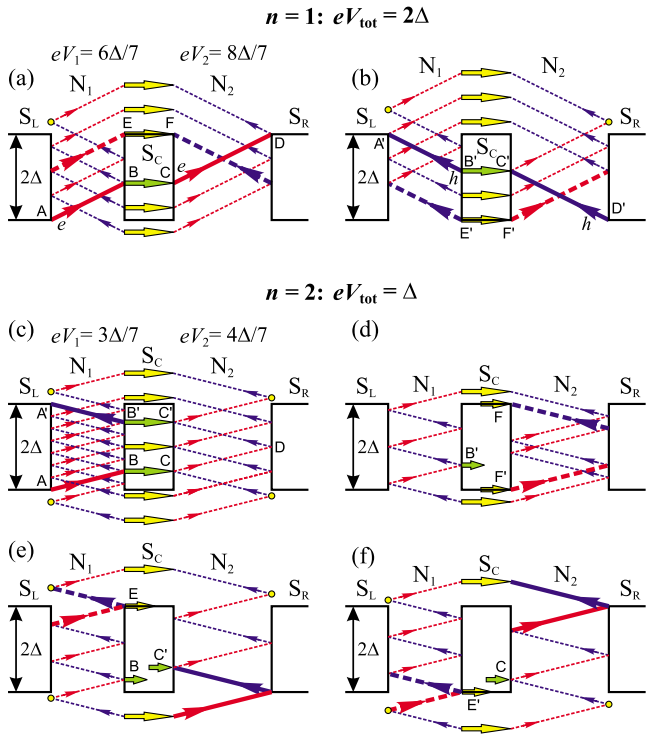

FIG. 1. (Color online) Diagrams of the SAT processes for $n=1$, panels (a) and (b), and for $n=2$, panels (c)–(f) given by Eq. (1). The normal resistances ratio is $R_1/R_2=3/4$ (depicted as 3/4 ratio of the respective lengths of the normal regions). Synchronization of energies of the incident and emitted quasiparticles within the central island S_C (shown by thick arrows) aligns MAR staircases in the normal parts N_1 and N_2 and results in a polygon trajectory for charge transfer. Segments ABCD [panel (a)] and D′C′B′A′ [panel (b)] starting and ending at the points of singularity in the density of states at energies $\varepsilon=\pm\Delta$ at the electrodes S_L and S_R correspond to the electron and hole trajectories, respectively. Dashed thick lines emphasize the segments passing through the singularities at edges of the gap of the central island S_C and thus amplifying the SAT process as compared to individual MARs. Segments not passing through the density-of-states singularity points are shown by dotted lines. Circles denote the above-the-gap Andreev reflections. Panel (c) shows the contribution into the formation of the second harmonic from the trajectory that starts with the emission of the quasiparticle from the point A at S_L and ends by absorption of the hole at point A′ at the same superconducting island. The panels (d)–(f) represent one diagram which is decomposed into three panels for the convenience. A quasiparticle hitting S_C at point B′ on panel (d) is synchronized with the quasiparticle emitting from point C′ of S_C on panel (e) [simultaneously, the inverse transfer, via the hole hitting S_C at C′ and continuing further from B′ takes place]. Analogously, the hole thrusting S_C at the edge of the gap (point F) on panel (f) is synchronized with the quasiparticle arriving at point E shown on panel (e).

above-the-gap transmissions and Andreev reflections. The enhancement of the transmission as compared to the conventional MAR process is achieved due to involvement of additional density-of-states singular points at the central island. Thus, the main contribution into formation of the second subharmonic comes from the four diagrams shown in Figs. 1(c)–1(f). Apart from the main singularities [Eq. (1)], additional SAT satellite spikes appear at $V=(2\Delta/e)(p+q)/n$, where p/q is the irreducible rational approximation of the real number $r=R_1/R_2$ (we take $R_1<R_2$) and $n\geq(p+q)$.

III. SYSTEM AND THEORETICAL FORMALISM

We consider the charge transfer across an $S_LN_1S_CN_2S_R$ junction, where S_L, S_C, and S_R are superconducting islands with identical gap Δ. The normal parts N_1 and N_2 have, in general, different resistances and are the diffusive normal metals of lengths $L_{1,2}>\xi$, where ξ is the superconducting coherence length and $L_{1,2}>L_T$, $L_T=\sqrt{\hbar D_N/\varepsilon}$, where D_N is the diffusion coefficient in the normal metal. We assume the Thouless energy, $E_{Th}=\hbar D_N/L_{1,2}^2$, to be small, $E_{Th}\ll eV_{1,2},\Delta$, where $V_{1,2}$ are the partial voltage drops in normal parts, implying that the Josephson coupling between the superconducting islands is suppressed.[24] We let the energy relaxation length in the normal parts N_1 and N_2 be much larger than their sizes, thus quasiparticles may experience many incoherent Andreev reflections inside the normal regions. These conditions are referred to as incoherent regime[21,23] and correspond to common experimental situations.[11–20] We take the size of the central island $L_C\gg\xi$. This ensures that processes of subgap elastic cotunneling, direct Andreev tunneling,[25] and Coulomb blockade effects are irrelevant for the quasiparticle transport. At the same time L_C is assumed to be less than the charge imbalance length so that the coordinate dependence of the quasiparticle distribution functions across the island S_C is negligible. Additionally, the condition $\ell_\varepsilon\gg L_C$, where ℓ_ε is the energy relaxation length, implies that quasiparticles with energies $\varepsilon>\Delta$ traverse the superconducting island S_C without losing energy.

The current transfer across the SNSNS junction is described by quasiclassical Larkin-Ovchinnikov equations for the dirty limit,[26]

$$-i[\check{H}_{\rm eff}\circ,\check{\mathbf{G}}]=\nabla\check{\mathbf{J}},\quad \check{\mathbf{J}}\cdot\mathbf{n}=\frac{1}{2\sigma_S R}[\check{G}_S,\check{G}_N],\qquad(2)$$

where $\check{H}_{\rm eff}=\check{1}(i\hat{\sigma}_z\partial_t-\varphi\hat{\sigma}_0+\hat{\Delta})$, $\check{\mathbf{J}}=D\check{\mathbf{G}}\circ\nabla\check{\mathbf{G}}$ is the matrix current, the subscripts "S" and "N" stand for superconducting and normal materials, respectively, "$\circ$" is the time convolution, $\hat{\sigma}_i$ $(i=\{x,y,z\})$ are the Pauli matrices, $\hat{\Delta}=i\hat{\sigma}_x\,\mathrm{Im}\,\Delta+i\hat{\sigma}_y\,\mathrm{Re}\,\Delta$, and R is the resistance of an NS interface. The diffusion coefficient D assumes the value D_N in the normal metal and the value D_S in the superconductor, and φ is the electrical potential which we calculate self-consistently. The unit vector $\mathbf{n}$ is normal to the NS interface and is assumed to be directed from N to S. The momentum averaged Green's functions $\check{\mathbf{G}}(\mathbf{r},t,t')$ are 2×2 matrices in a Keldysh space. Each element of the Keldysh matrix, labeled with a hat sign, is, in its turn, a 2×2 matrix in the electron-hole space,

$$\check{\mathbf{G}}=\begin{pmatrix}\hat{G}^{\rm R} & \hat{G}^{\rm K}\\ 0 & \hat{G}^{\rm A}\end{pmatrix};\quad \hat{G}^{\rm R(A)}=\begin{pmatrix}\mathcal{G}^{\rm R(A)} & \mathcal{F}^{\rm R(A)}\\ \tilde{\mathcal{F}}^{\rm R(A)} & \tilde{\mathcal{G}}^{\rm R(A)}\end{pmatrix},\qquad(3)$$

$\mathbf{r}$ is the spatial position, and t and t' are the two time arguments. The Keldysh component of the Green's function is

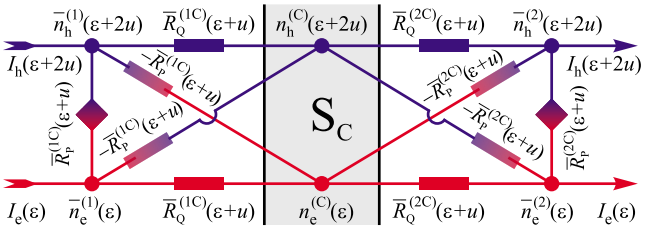

FIG. 2. (Color online) Effective circuit representing current conversion at the interfaces of the central superconducting island S_C. Resistors, R_P and R_Q stand for an Andreev and a normal processes, respectively.

parametrized as[26] $\hat{G}^K=\hat{G}^R\circ\hat{f}-\hat{f}\circ\hat{G}^A$, where $\hat{f}$ is the distribution function matrix, diagonal in Nambu space, $\hat{f}\equiv\mathrm{diag}\,[1-2n_e,1-2n_h]$, $n_{e(h)}$ is the electron (hole) distribution function. In equilibrium $n_{e(h)}$ becomes the Fermi function. And, finally, the Green's function satisfies the normalization condition $\check{\mathbf{G}}^2=\check{1}$.

The edge conditions closing Eq. (2) are given by the expressions for the Green's functions in the bulk of the left (L) and right (R) superconducting leads

$$\check{\mathbf{G}}_{L(R)}(t,t')=e^{-i\mu_{L(R)}t\hat{\sigma}_z/\hbar}\check{\mathbf{G}}_0(t-t')e^{i\mu_{L(R)}t'\hat{\sigma}_z/\hbar},$$

the chemical potentials are $\mu_L=0$ and $\mu_R=eV$. Here, $\check{\mathbf{G}}_0(t)$ is the equilibrium bulk BCS Green's function.

The current density is expressed through the Keldysh component of $\check{\mathbf{J}}$ as

$$\mathcal{I}(t,\mathbf{r})=\frac{\pi\sigma_N}{4}\mathrm{Tr}\,\hat{\sigma}_z\hat{J}^K(t,t;\mathbf{r})=\frac{1}{2}\int d\varepsilon[I_e(\varepsilon)+I_h(\varepsilon)], \quad (4)$$

where the spectral currents I_e and I_h are the time Wigner transforms of top and bottom diagonal elements of the matrix current $\check{\mathbf{J}}^{(K)}$, representing electron and hole quasiparticle currents, respectively. In the bulk of a normal metal $I_e=\sigma_N\nabla n_e$ and $I_h=\sigma_N\nabla n_h$.

The distribution functions of quasiparticles at the central island S_C are the nonequilibrium ones, implying the nonequilibrium boundary conditions at corresponding NS interfaces. To deal with it, we define the quasiparticle spectral currents at the interfaces as the Keldysh component of Eq. (2), and the resulting nonequilibrium boundary conditions acquire a form of Kirchhoff's laws for the circuit shown in Fig. 2. The electron and hole distribution functions take the role of voltages at the nodes. To illustrate our technique, we write down the equation for an electronic spectral current flowing into the lower left corner node (Kirchhoff's laws at the other corner nodes have a similar form)

$$I_e(\varepsilon)=\frac{1}{\bar{R}_Q^{(1C)}(\varepsilon+u)}[n_e^{(C)}(\varepsilon)-\bar{n}_e^{(1)}(\varepsilon)]-\frac{1}{\bar{R}_P^{(1C)}(\varepsilon+u)}[n_h^{(C)}(\varepsilon+2u)-\bar{n}_e^{(1)}(\varepsilon)]+\frac{1}{\bar{R}_P^{(1C)}(\varepsilon+u)}[\bar{n}_h^{(1)}(\varepsilon+2u)-\bar{n}_e^{(1)}(\varepsilon)]. \quad (5)$$

The interjacent resistances, $\bar{R}_{Q(P)}$, are defined as $\bar{R}_{Q(P)}^{-1}(\varepsilon)=\{\bar{R}_-^{-1}(\varepsilon)\pm\bar{R}_+^{-1}(\varepsilon)\}/2$, where $\bar{R}_\pm(\varepsilon)$ are the special functions characterizing transparencies of the interfaces and tabulated in Ref. 21. At high energies, $|\varepsilon|\gg\Delta$, $\bar{R}_+(\varepsilon)\to\bar{R}_-(\varepsilon)$; at small energies, $|\varepsilon|\ll\Delta$, $\bar{R}_-(\varepsilon)$ diverges while $\bar{R}_+(\varepsilon)-\bar{R}_-(\varepsilon)$ remains finite; and there are singularities in $\partial_\varepsilon\bar{R}_\pm(\varepsilon)$ at $|\epsilon|=\Delta$, which are of the same origin as those in the BCS density of states and reflect the fact that quasiparticles cannot penetrate the superconductor below the gap. The "bars" indicate that the respective resistances and the distribution functions are "renormalized"[21] by the proximity effect.

To derive the current-voltage characteristics for the general case of an asymmetric nonequilibrium SNSNS junction with different resistances of the normal regions, we construct a nonequilibrium circuit theory allowing for an analytical solution of the nonlinear nonuniform matrix Eq. (2) for Keldysh-Nambu Green's functions. The diagrammatic mapping of Eq. (2) is realized by an equivalent circuit shown in Fig. 3. The Kirchhoff's equations for the potential distribution in the circuit of Fig. 3 give the recurrent relations,

$$\mathcal{R}(\varepsilon,-u,-V)I_h(\varepsilon)-\rho^{(\circ)}(\varepsilon-u)I_e(\varepsilon-2u)-\rho^{(\triangleright)}(\varepsilon)I_e(\varepsilon)-\rho^{(\triangleleft)}(\varepsilon-V)I_e(\varepsilon-2V)=n_F(\varepsilon)-n_F(\varepsilon-V), \quad (6)$$

$$\mathcal{R}(\varepsilon,u,V)I_e(\varepsilon)-\rho^{(\circ)}(\varepsilon+u)I_h(\varepsilon+2u)-\rho^{(\triangleright)}(\varepsilon)I_h(\varepsilon)-\rho^{(\triangleleft)}(\varepsilon+V)I_h(\varepsilon+2V)=n_F(\varepsilon+V)-n_F(\varepsilon), \quad (7)$$

where the electric potential u of the S_C island is calculated self-consistently from the electroneutrality condition, $u=(\pi/8)\mathrm{Tr}\,\hat{G}^K$. The effective resistance is $\mathcal{R}=R_1+R_2+\rho^{(\triangleright\circ\triangleleft)}$, where $\rho^{(\triangleright\circ\triangleleft)}=(1/2)\Sigma_{\alpha=\pm}\{\bar{R}_{\alpha,\varepsilon}^{(1L)}+\bar{R}_{\alpha,\varepsilon+u}^{(1C)}+\bar{R}_{\alpha,\varepsilon+u}^{(2C)}+\bar{R}_{\alpha,\varepsilon+V}^{(2R)}\}$, $\rho^{(\circ)}=(1/2)\{\bar{R}_+^{(1C)}+\bar{R}_+^{(2C)}-\bar{R}_-^{(1C)}-\bar{R}_-^{(2C)}\}$, $\rho^{(\triangleleft)}=(1/2)\{\bar{R}_+^{(2R)}-\bar{R}_-^{(2R)}\}$, and $\rho^{(\triangleright)}=(1/2)\{\bar{R}_+^{(1L)}-\bar{R}_-^{(1L)}\}$. Solutions of Eqs. (6) and (7) yield the required I-V characteristics for an asymmetric SNSNS junction. To verify our formulas we note that at large quasiparticle energies, $|\varepsilon|\gg\Delta$, the total resistance $\mathcal{R}$ reduces to the normal resistance of the array, whereas $\rho^{(\triangleleft)}$, $\rho^{(\triangleright)}$, and $\rho^{(\circ)}$ vanish. Then we find from Eqs. (6) and (7) that $I_h(\varepsilon)=[n_F(\varepsilon)-n_F(\varepsilon-V)]/\mathcal{R}$ and $I_e(\varepsilon)=[n_F(\varepsilon+V)-n_F(\varepsilon)]/\mathcal{R}$, which together with Eq. (4) reproduce Ohm's law, $\mathcal{I}=V/\mathcal{R}$. The constructed diagram, Fig. 3, is an elemental building unit for a general nonequilibrium quantitative theory of SNS arrays comprised of many SNS junctions.

IV. RESULTS AND DISCUSSION

The calculation of the current-voltage characteristics $\mathcal{I}(V)$ requires the numerical solution of the recurrent relations, Eqs. (6) and (7). To this end, we have developed a computational scheme allowing to bypass instabilities caused by the nonanalytic behavior of the spectral currents $I_{e(h)}(\varepsilon)$. We first fix some chosen energy ε, identify the set of energies connected through the equations in the given energy interval, and solve the resulting subsystem of equations. We then repeat the procedure, until the required energy resolution of

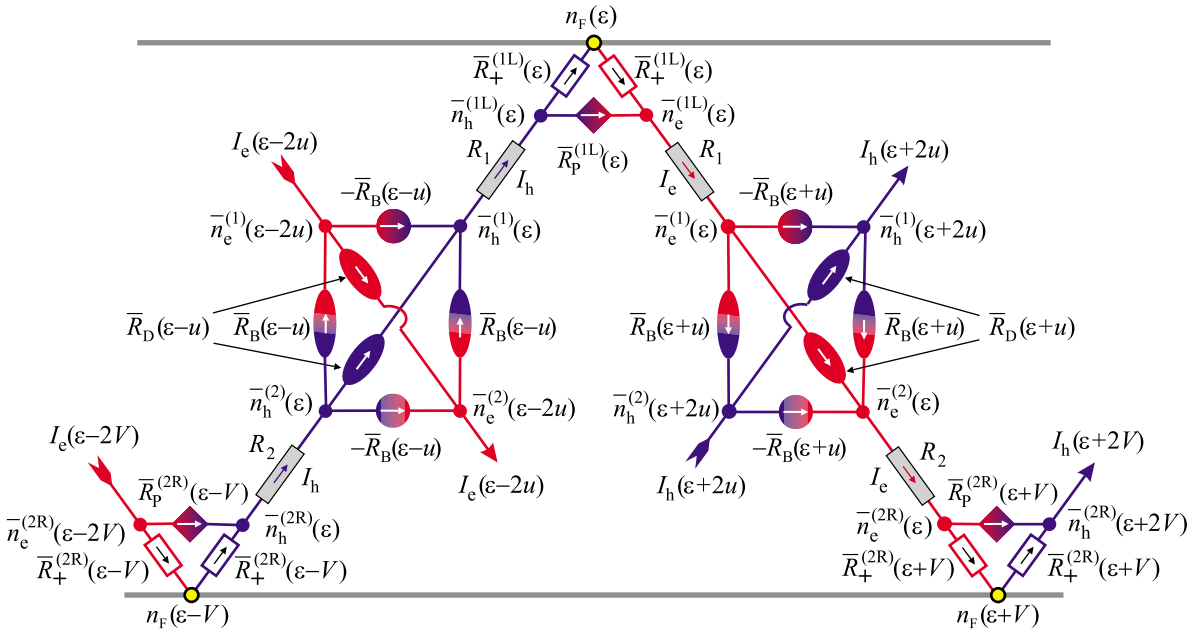

FIG. 3. (Color online) Effective circuit for an SNSNS junction. The elemental blocks given in Fig. 2 are simplified by introduction of resistors $\bar{R}_{D(B)}^{-1}=(1/2)\{[\bar{R}_+^{(1C)}+\bar{R}_+^{(2C)}]^{-1}\pm[\bar{R}_-^{(1C)}+\bar{R}_-^{(2C)}]^{-1}\}$ represent Andreev and normal processes at the NS interfaces of the central island.

$\delta\varepsilon=10^{-5}\Delta$ is achieved. Typically, up to 10^6 linear equations had to be solved for every given voltage but the complexity of the coupled subsystem depends on the commensurability of u and V.

Figure 4 shows the comparative results for the SNSNS junction and two SNS junctions in series. The latter corresponds to the case where the size of the central island well exceeds the energy relaxation length, $L_C>\ell_\varepsilon$. We display the differential resistances as functions of the applied voltage, which demonstrate the singularities in Andreev transmission more profoundly than the *I-V* curves. There is a pronounced SAT spike in the dV/dI for an SNSNS junction at $V_{tot}=2\Delta/e$. The spike appears irrespectively of the partial voltage drops in the normal regions and is absent in the corresponding curves representing two individual MAR processes at the junctions SN_1S and SN_2S.

To connect to experimental observations of Refs. 2–6, we show now that high subharmonic SAT resonances become even more pronounced with the growth of the number of SNS junctions in the system. Indeed, let us assume that the resistances of the normal islands in a chain of SNS junctions are randomly scattered around their average value R_0 and follow Gaussian statistics with the standard deviation $\sigma_R=\sigma R_0$, where σ is dimensionless. Then the dispersion of the single junction MAR resonant voltages is characterized by the same σ, and the MAR features get smeared. Let us now consider the situation where nth subharmonic results from the distribution of the bias $V_{tot}=2\Delta/e$ among the n successive islands. Then the total standard deviation of the voltage drop grows as $\sqrt{n}$ because of the statistical summation. Thus the voltage deviation *per one island* is $\propto 1/\sqrt{n}$, i.e., the dispersion of the distribution of V_n drops with increasing n: $\sigma_{SAT}=\sigma/\sqrt{n}$. As a result the high subharmonic spikes at voltages V_n per junction due to the SAT become more sharp and pronounced (in contrast to MAR-induced features) in large systems—in a full agreement with the experimental observations.[2–4]

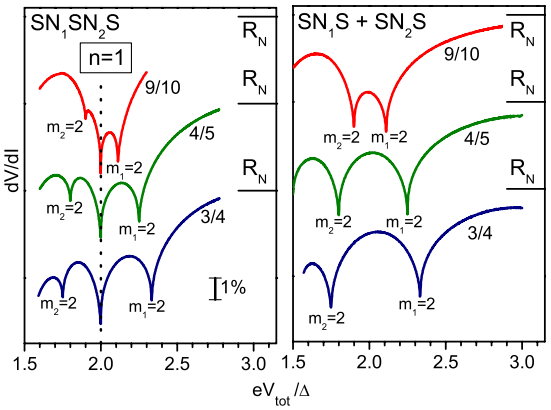

FIG. 4. (Color online) Left panel: differential resistances as functions of the applied voltage V_{tot} [around $n=1$ in Eq. (1)] for the SN_1SN_2S junction. The fractions 3/4, 4/5, and 9/10 represent the ratios of resistances of the normal regions, R_1/R_2. dV/dI of SN_1SN_2S junction demonstrates the pronounced SAT spike at $V_{tot}=2\Delta/e$, irrespectively of the partial voltage drops. The SAT spike is sandwiched between the two spikes corresponding to individual MAR processes occurring at junctions SN_1S and SN_2S for $m_1,m_2=2$. The voltage positions of these features depends on R_1/R_2. Right panel: the corresponding $dV/dI(V_1+V_2)$ for two SN_1S and SN_2S junctions in series as they would have appeared in absence of the synchronization process, i.e., when $L_C>\ell_\varepsilon$. These dV/dI were calculated following Ref. 21 (with transmissivity $W=1$). The calculations are done at $T=0$; at finite temperatures the spikes are more smeared in accord with the smoothening of the BCS singularities at the edge of the superconducting gap.

V. CONCLUSIONS

In conclusion, we have developed a nonequilibrium theory of charge transfer across an SNSNS array and found that the central island acts as Andreev *retransmitter*. We have shown that the nonequilibrium transport through the array is governed by synchronized Andreev transmission with correlated conversion processes at the NS interfaces. The constructed theory is a fundamental building unit for a general quantitative description of a large system consisting of many SNS junctions.

ACKNOWLEDGMENTS

We thank A. N. Omelyanchuk for helpful discussions. The work was supported by the U.S. Department of Energy, Office of Science under Contract No. DE-AC02-06CH11357, by the Russian Foundation for Basic Research (Grants No. 10-02-00700 and No. 09-02-01205), the Dynasty, and the Programs of the Russian Academy of Science.

[1] R. S. Newrock, C. J. Lobb, U. Geigenmüller, and M. Octavio, in *Solid State Physics*, edited by H. Ehrenreich and F. Spaepen (Academic Press, San Diego, 2000), Vol. 54, p. 263.
[2] T. I. Baturina, Z. D. Kvon, and A. E. Plotnikov, Phys. Rev. B **63**, 180503(R) (2001).
[3] T. I. Baturina, Yu. A. Tsaplin, A. E. Plotnikov, and M. R. Baklanov, JETP Lett. **81**, 10 (2005).
[4] T. I. Baturina, A. Yu. Mironov, V. M. Vinokur, N. M. Chtchelkatchev, A. Glatz, D. A. Nasimov, and A. V. Latyshev, Physica C (to be published).
[5] T. I. Baturina, D. R. Islamov, and Z. D. Kvon, JETP Lett. **75**, 326 (2002).
[6] J. Fritzsche, R. B. G. Kramer, and V. V. Moshchalkov, Phys. Rev. B **80**, 094514 (2009).
[7] A. F. Andreev, Zh. Eksp. Teor. Fiz. **46**, 1823 (1964) [Sov. Phys. JETP **19**, 1228 (1964)].
[8] T. M. Klapwijk, G. E. Blonder, and M. Tinkham, Physica B & C **109-110**, 1657 (1982).
[9] M. Octavio, M. Tinkham, G. E. Blonder, and T. M. Klapwijk, Phys. Rev. B **27**, 6739 (1983).
[10] K. Flensberg, J. B. Hansen, and M. Octavio, Phys. Rev. B **38**, 8707 (1988).
[11] J. M. Rowell and W. E. Feldmann, Phys. Rev. **172**, 393 (1968).
[12] P. E. Gregers-Hansen, E. Hendricks, M. T. Levinsen, and G. R. Pickett, Phys. Rev. Lett. **31**, 524 (1973).
[13] W. M. van Huffelen, T. M. Klapwijk, D. R. Heslinga, M. J. de Boer, and N. van der Post, Phys. Rev. B **47**, 5170 (1993).
[14] A. W. Kleinsasser, R. E. Miller, W. H. Mallison, and G. B. Arnold, Phys. Rev. Lett. **72**, 1738 (1994).
[15] E. Scheer, P. Joyez, D. Esteve, C. Urbina, and M. H. Devoret, Phys. Rev. Lett. **78**, 3535 (1997).
[16] J. Kutchinsky, R. Taboryski, T. Clausen, C. B. Sørensen, A. Kristensen, P. E. Lindelof, J. Bindslev Hansen, C. Schelde Jacobsen, and J. L. Skov, Phys. Rev. Lett. **78**, 931 (1997).
[17] A. Frydman and R. C. Dynes, Phys. Rev. B **59**, 8432 (1999).
[18] T. Hoss, C. Strunk, T. Nussbaumer, R. Huber, U. Staufer, and C. Schönenberger, Phys. Rev. B **62**, 4079 (2000).
[19] T. I. Baturina, Z. D. Kvon, R. A. Donaton, M. R. Baklanov, E. B. Olshanetsky, K. Maex, A. E. Plotnikov, and J. C. Portal, Physica B **284-288**, 1860 (2000).
[20] Z. D. Kvon, T. I. Baturina, R. A. Donaton, M. R. Baklanov, K. Maex, E. B. Olshanetsky, A. E. Plotnikov, and J. C. Portal, Phys. Rev. B **61**, 11340 (2000).
[21] E. V. Bezuglyi, E. N. Bratus', V. S. Shumeiko, G. Wendin, and H. Takayanagi, Phys. Rev. B **62**, 14439 (2000). Here superconductors were assumed to be in a local equilibrium so that $I_e(\varepsilon) = I_h(\varepsilon - V)$ was satisfied. This approach that was extended on symmetric SNSNS by Chtchelkatchev (Ref. 22) leads to an equivalent circuit with the infinite number of elements for a general nonsymmetric SNS array.
[22] N. M. Chtchelkatchev, JETP Lett. **83**, 250 (2006).
[23] J. C. Cuevas, J. Hammer, J. Kopu, J. K. Viljas, and M. Eschrig, Phys. Rev. B **73**, 184505 (2006).
[24] P. Dubos, H. Courtois, B. Pannetier, F. K. Wilhelm, A. D. Zaikin, and G. Schön, Phys. Rev. B **63**, 064502 (2001).
[25] G. Deutscher and D. Feinberg, Appl. Phys. Lett. **76**, 487 (2000).
[26] A. I. Larkin and Y. N. Ovchinnikov, Sov. Phys. JETP **41**, 960 (1975); **46**, 155 (1977).